Available online at www.sciencedirect.com

SciVerse ScienceDirect

Ceramics International 39 (2013) 7809–7815

CERAMICS INTERNATIONAL

www.elsevier.com/locate/ceramint

The effect of EEMAO processing on surface mechanical properties of the TiO_2–ZrO_2 nanostructured composite coatings

K. Yousefipour[a], A. Akbari[a], M.R. Bayati[b,*]

[a]Faculty of Materials Engineering, Sahand University of Technology, Tabriz 51335-1996, Iran
[b]Department of Materials Science and Engineering, North Carolina State University, EB-1, Raleigh, NC 27695-7907, USA

Received 2 March 2013; received in revised form 4 March 2013; accepted 12 March 2013
Available online 20 March 2013

Abstract

We report fabrication of TiO_2–ZrO_2 nanostructured composite coatings by EPD-Enhanced MAO (EEMAO) technique on titanium substrates where especial emphasis was placed on improving the surface hardness of the substrates and establishing a microstructure-property correlation. Based on the XRD and the EDX results, the layers consisted of anatase, rutile, monoclinic zirconia, and tetragonal zirconia. It was observed that the anatase/rutile and tetragonal/monoclinic zirconia rations increased with the processing time and the electrolyte concentration. The zirconia content also increased with the processing time and the electrolyte concentration. XPS technique was also employed to further confirm the surface chemical composition and stoichiometry of the layers. A uniform distribution of zirconia across the titania matrix was evident in the SEM images. The surface hardness of the TiO_2-ZrO_2 composite layers was observed to increase with the zirconia concentration. Employing EEMAO technique, the surface harness of the titanium substrates was successfully improved from ~190 Hv to ~700 Hv.

Keywords: C. Hardness; Titania; Zirconia; Nanostructures; Composite

1. Introduction

Titanium and its alloys are extensively used in many high-tech technologies including aerospace [1], biomedical [2], chemical and petrochemical [3], and automotive [4] due to their high strength-to-weight ratio, excellent corrosion resistance, biocompatibility, and low mass-to-volume ratio. Titanium based alloys are usually considered to be resistant enough in corrosive environments; however, their abrasive resistance and surface mechanical properties are not favorable limiting their practical applications. As of today, finding a way to improve the wear resistance and surface hardness of titanium parts has been the main focus of many research activities [5–10]. Applying hard coatings, such as TiO_2, seems to be an effective way to improve surface mechanical properties of titanium components. TiO_2 with its unique properties has gained wide attentions as a hard coating to enhance tribologic characteristics of surface of titanium parts. To further enhance the mechanical characteristics of titania, it is proposed to combine it with other hard oxides such as ZrO_2 which has favorable chemical and thermal stability, high strength and fracture toughness, high wear and corrosion resistance, and very high hardness [11–13]. The most attractive feature of composite films is that the properties of the composite materials can be precisely manipulated through a simple control over the composition of the systems. In addition, the composite system often exhibits enhanced mechanical and thermal properties than the two participating components [14,15].

Composite ZrO_2–TiO_2 films with several advantages like enhance the thermal stability [16], wear resistance [17], corrosion resistance [18] frictional behavior [17] and hardness [19]. In this study, micro-arc oxidation (MAO) and electrophoretic deposition (EPD) methods were combined and used to fabricate TiO_2–ZrO_2 layers. Although superior corrosion and thermal barrier properties of the TiO_2–ZrO_2 layers have been proved, but the mechanical properties have not been evaluated yet [20]. This feature will be discussed in this report.

MAO is a novel anodic oxidation technique to modify the surface characteristics of valve metals. This technique has gained attentions in improving the tribologic properties of the

*Corresponding author. Tel.: +1 919 917 6962; fax: +1 919 515 7724.
E-mail address: mbayati@ncsu.edu (M.R. Bayati).

0272-8842/$ - see front matter © 2013 Elsevier Ltd and Techna Group S.r.l. All rights reserved.
http://dx.doi.org/10.1016/j.ceramint.2013.03.041

metallic components. More details on the mechanism of the MAO process can be found in the literature [21–24]. The MAO grown coatings exhibit favorable interfacial adhesion, high hardness, and excellent tribologic performance. The porous nature of the MAO fabricated samples is very much suitable for lubricant retention. Electrophoretic deposition (EPD) is an electrochemical technique where charged particles, dispersed in a solution, are deposited onto an oppositely charged electrode. The charged particles are accelerated toward the electrodes by the electric field between the poles of the electrochemical cell. EPD is a simple and inexpensive technique making it possible to synthesize a wide range of coatings with varying morphologies and chemical compositions. This method has been developed to fabricate a variety of dense, nanostructured functional layers with desirable thickness. Components with complicated geometries can be coated via the EPD method evenly, due to the favorable throwing power [25–29]. So far, nanocomposite layers with enhanced properties have been successfully fabricated by EPD process; suspensions of ZrO_2 [30], SiO_2 [31], carbon nanotubes [32], and alumina [33] nanoparticles were utilized as electrolyte.

In this study, we took the advantages of both MAO and EPD techniques to grow porous TiO_2–ZrO_2 composite layers on titanium substrates. The layers were grown under different conditions and characterized. The main focus was placed on the improvement of the surface hardness of titanium components. We could propose a correlation between the processing parameters, structure, and the surface mechanical properties of the titanium substrates.

2. Experimental procedure

Titanium foils, with dimensions of 30 mm × 10 mm × 2 mm, were used as substrate and connected to the positive pole of the power supply as anode. Table 1 shows chemical composition of the titanium substrates. Prior to EEMAO processing, the substrates were cleaned through mechanical polishing by sand papers #80 to #2500 until a mirror level, rinsing in distilled water, ultrasonic cleaning in acetone for 15 min at room temperature, and rinsing in distilled water. Finally, the substrates were dried by an air jet. The cleaned substrates were EEMAO processed in an aqueous solution of sodium phosphate ($Na_3PO_4 \cdot 12H_2O$, Merck) and zirconia nanoparticles. Chemical composition of the utilized electrolytes is presented in Table 2. After mixing the components, the electrolyte was stirred for 24 h at 100 RPM in order to completely disperse the zirconia nanoparticles. Temperature of the electrolyte during the EEMAO processing was kept constant at about 70 °C using water and ice. A stainless steel cylinder surrounding the titanium anodes was employed as cathode to provide a uniform distribution of the electrical field onto the surface of the anodes.

Phase structure of the samples was studied by a D8 ADVANCE-BRUKER AXS X-ray diffractometer (Cu-Kα radiation). Morphological investigations were carried out by a CamScan MV2300 SEM/EDX. A VG Microtech XPS (Twin anode, XR3E2 X-ray source, using Al Kα = 1486.6 eV) was employed to study the stoichiometry and surface chemical composition of the samples. All interpretations were referenced to the C(1s) core level at 285.0 eV. Finally, hardness of the layers was measured by a MDPEL-M400 GL microhardness tester.

3. Results and discussion

3.1. Phase structure and chemical composition

θ–2θ XRD diffraction patterns of the composite layers grown at the voltage of 425 V for 10 min in different electrolytes are depicted in Fig. 1 where formation of anatase TiO_2, rutile TiO_2, monoclinic zirconia, and tetragonal zirconia phases is evident. A couple of features in this figure are worth nothing. First, the rutile/anatase relative content increased when a thicker electrolyte (electrolyte C) was used. The electrical resistance of the electrolyte decreases when its concentration increases and, thus, the electrical conductivity of the MAO cell increases. This phenomenon give rises to a higher electric current passing through the cell at a constant voltage. Therefore, more heat is generated and the anode (substrate) warms up due to higher electrical current [34]. Because of this extra heat, the anatase meta-stable phase transforms into the rutile stable phase. Local temperature at the discharge spots reach 10^3–10^4 K [34,35]. Of course, the overall temperature of the substrate is raised to about 400–800 °C, depending on the process parameters. It is worth mentioning that anatase transforms into the rutile polymorph at about 600–800 °C [36,37]. Second, the XRD characteristic peaks of tetragonal and monoclinic zirconia intensify when a thicker electrolyte was utilized. Two reasons can be proposed for this behavior. In the thicker electrolytes, more zirconia particles are available, so they need to diffuse a shorter length to reach the substrate leading to the deposition of more zirconia particles on the growing layer at a constant voltage and processing time. Moreover, the electrolyte is agitated by

Table 2
Chemical composition of the utilized electrolytes.

No.	Component	
	Na_3PO_4 (g l^{-1})	ZrO_2 (g l^{-1})
A	5	0
B	5	0.5
C	5	2

Table 1
Elemental chemical composition of the as-received titanium substrates.

Element	Ti	O	Al	Si	Mn	Fe
Wt%	80.02	17.08	1.02	0.92	0.57	0.38

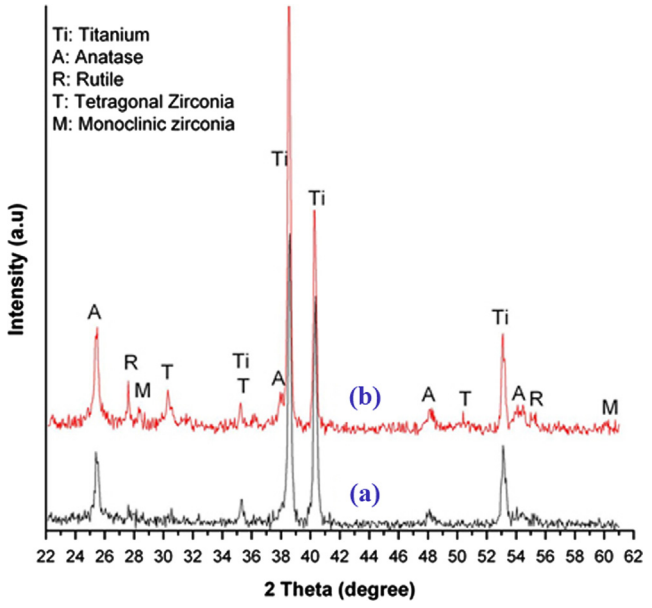

Fig. 1. XRD patterns of the composite layers grown in: (a) electrolyte B and (b) electrolyte C for 10 min.

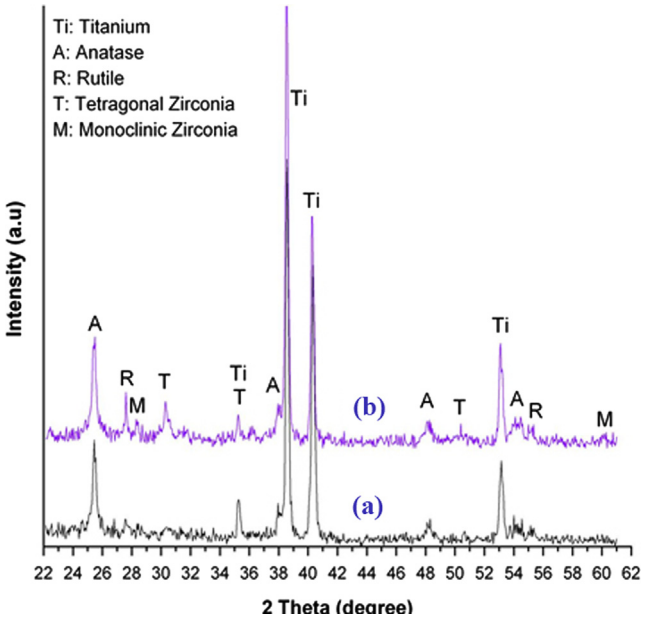

Fig. 2. XRD patterns on the composite layers grown in electrolyte C for different times: (a) 5 and (b) 10 min.

the stronger electric sparks forming at the higher electrical currents facilitating the diffusion in the electrolyte and increasing the zirconia content in the layers. Third, the relative content of tetragonal zirconia to monoclinic zirconia increases when thicker electrolyte is used. As it was already discussed, the layer grows at a higher temperature when a thicker electrolyte is used. This phenomenon results in the phase transformation of monoclinic zirconia to the tetragonal zirconia. This phase transformation improves the mechanical properties of the coatings combined with zirconia. Since a basic electrolyte was utilized, OH^- anions get attached to the defects sites (like oxygen vacancies) on the zirconia particles surface resulting in the formation of negatively charged particles. These particles move toward the anode due to the electrical field between anode and cathode.

The effect of growth time on phase structure of the TiO_2–ZrO_2 composite layers grown in the electrolyte C was also investigated. Fig. 2 shows the XRD patterns of the samples fabricated for 5 and 10 min., while other growth variables were kept constant. At longer growth times, thicker layers form, so it is expected that the intensity of all peaks increases. However, as is observed, the rutile peak gets more intense, while the intensity of the anatase peak is constant. This behavior is interpreted based on the dependence of substrate temperature upon the processing time. A longer growth time gives rise to the generation of more heat and, thus, phase transformation of the anatase phase into the rutile phase. Intensity of the ZrO_2 peaks also increases for the sample grown for 10 min indicating that more zirconia particles were deposited. Besides, the peak intensity of the tetragonal zirconia increases at longer growth times due to phase transformation of the monoclinic zirconia to the tetragonal zirconia, as discussed earlier.

Increasing the zirconia content of the layers with the growth time and the electrolyte concentration was further ascertained by EDX technique results of which are depicted in Fig. 3. Study on the chemical composition of the composite layers was completed by XPS characterization (Fig. 4). The C(1s) core level binding energy at 285.0 eV was used as reference to interpret the results. The XPS investigation was performed on the layer grown in the electrolyte C for 10 min. The O(1s) core level binding energy is depicted in Fig. 4a which was deconvoluted to 4 distinct peaks representing that there are 4 different O-bindings in the layers. Existence of water molecules on the surface is revealed by peak A, located at the binding energies of 533.7 eV. Since the layers were porous and fabricated in aqueous solutions, water may be trapped in the pores. Peak B, at the binding energy of 532.2 eV, represents the hydroxyl groups. Free surface of the oxide materials are always hydrated in the atmosphere. Therefore, the chemisorbed hydroxyl groups are always seen in the XPS patterns obtained from the oxide films. Peak C, with a binding energy of 531.0 eV, is attributed to the oxygen in nonstoichiometric zirconium oxides [38]. Peak D, at the binding energy of 529.7 eV, represents oxygen anions in the lattice of oxides, e.g. ZrO_2 and TiO_2. Fig. 4b shows the Ti($2p_{3/2}$) core level binding energy. The peak fitting was performed with only 1 component with a binding energy of 458.7 eV, assigned to the Ti^{4+} cations in Ti–O bonds in TiO_2. The Zr(3d) core level binding energy is shown in Fig. 4c. This peak has 2 components which are attributed to its spin orbit splitting, i.e. Zr($3d_{3/2}$) and Zr($3d_{5/2}$). Peaks A and B with binding energies of 185.4 and 184.5, respectively, represent zirconia. Formation of ZrO_2 is also confirmed by the peaks C and D located at the binding energies of 182.4 and 183.8 eV. The only reason why ZrO2 is represented by 4 peaks is the deviation from the stoichiometry. These achievements are in good agreement with those reported by other researchers [38,39]. The peaks E and F, at the binding energies of 180.2 and 181.4 eV, represent existence of Zr^{2+} and formation of ZrO and probably some other non-stoichiometric zirconium oxides (Zr_xO_y).

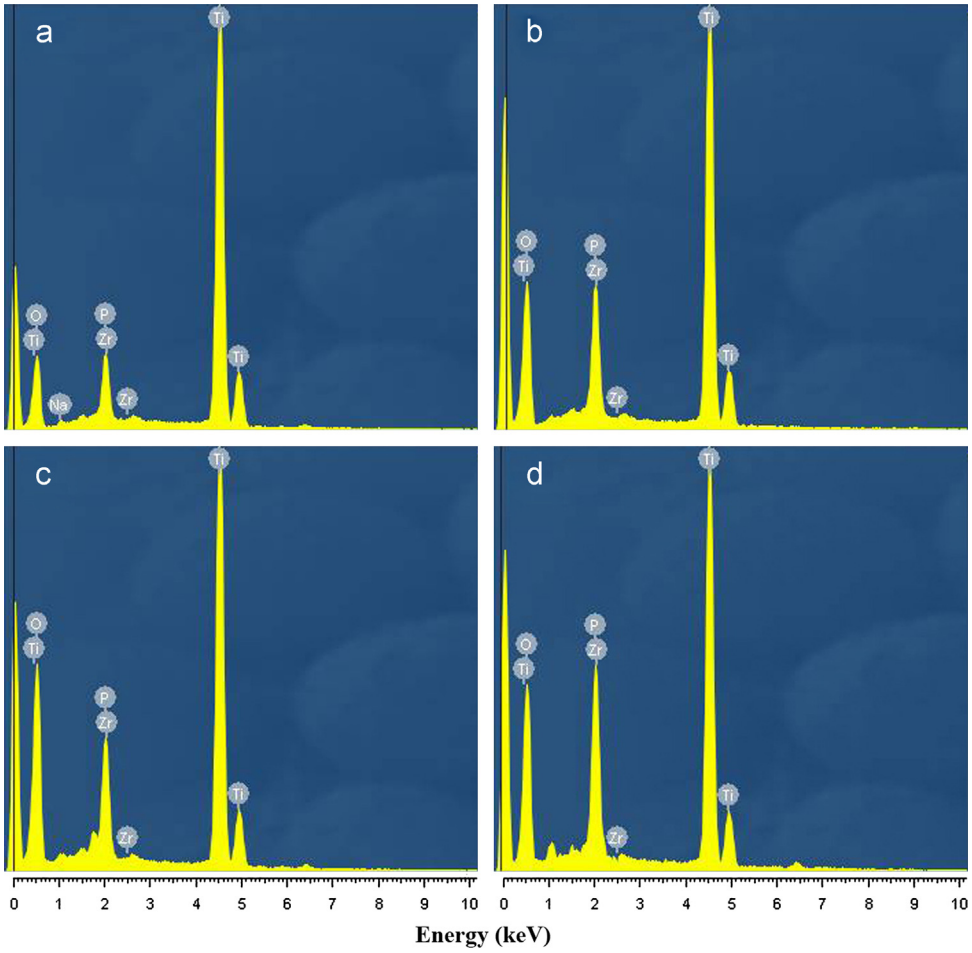

Fig. 3. EDX spectra of the layers grown at 425 V for different times in: (a) electrolyte B, for 5 min (b) electrolyte C, for 5 min (c) electrolyte B, for 10 min, and (d) electrolyte C, for 10 min.

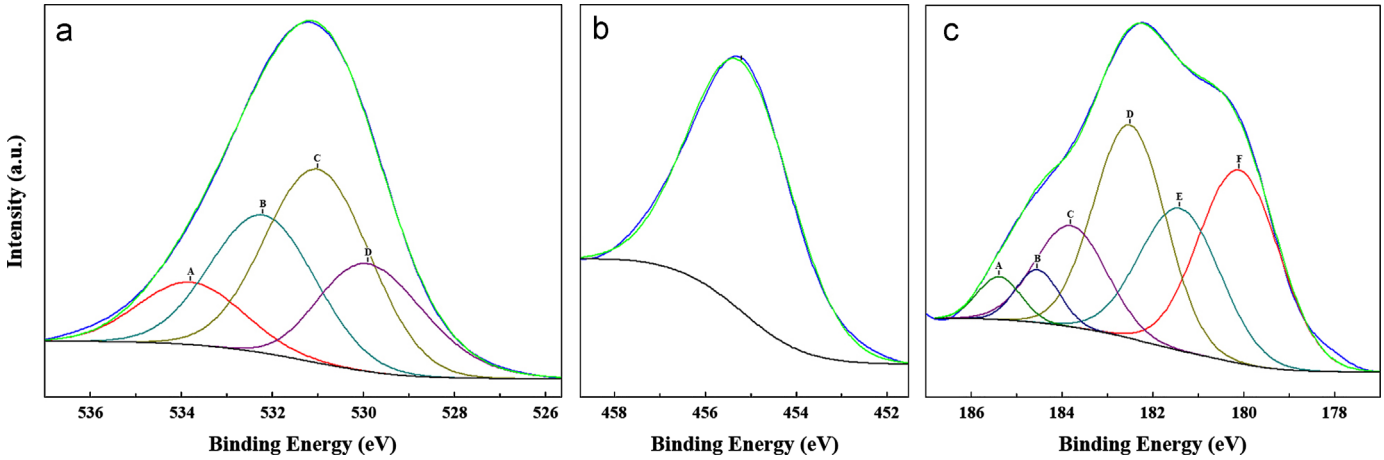

Fig. 4. XPS binding energies of: (a) O(1s), (b) Ti($2p_{3/2}$), and (c) Zr(3d) core levels.

Since ZrO_2 phase was detected by both XRD and XPS techniques, it is deduced that they have formed not only on the surface, but also in the bulk. The ZrO_2 particles are negatively charged, when they are dispersed in a basic solution. The negatively charged particles are accelerated toward the anode due to the electric field between the poles of the MAO cell. More details on the growth mechanism can be found in our previous works [40].

3.2. Morphology

SEM morphology of the pure TiO_2 and TiO_2–ZrO_2 layers are presented in Fig. 5. Formation of a porous structure, due to the electric sparks [41,42], is evident. As is also seen, size of the pores increases with the treatment time. We already showed that when structural pores form by electric sparks, those spots are more susceptible for successive electron

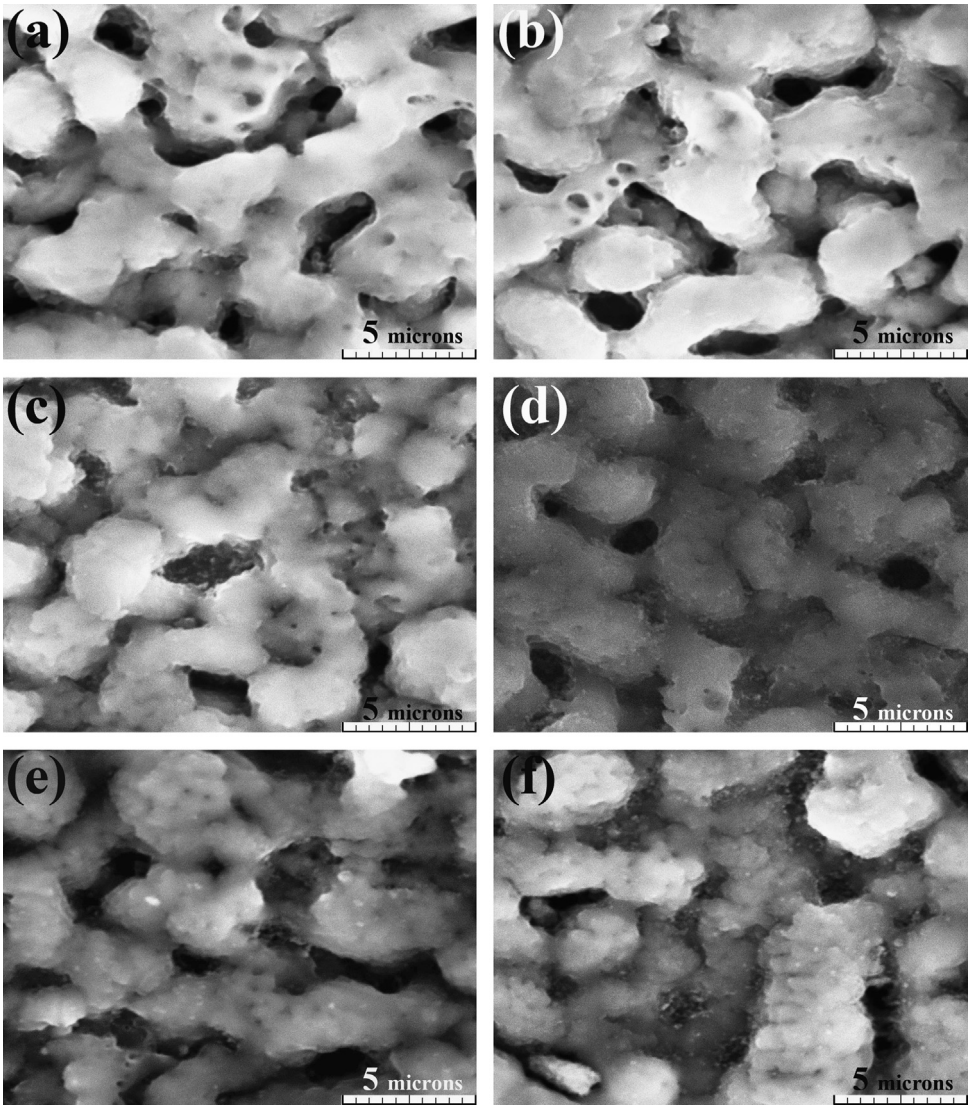

Fig. 5. SEM surface morphology of the composite layers grown under different conditions: (a) electrolyte A, 5 min, (b) electrolyte A, 10 min, (c) electrolyte B, 5 min, (d) electrolyte C, 5 min (e) electrolyte B, 10 min, and (f) electrolyte C, 10 min.

avalanches, since they have lower breakdown voltages, comparing to the nonporous areas [43]. Sequence of the electrical sparks makes the pores larger. Comparing the morphology of the pure TiO_2 layers with that of the composite layers reveals a uniform distribution of the zirconia nanoparticles. It is also clear that the concentration of the zirconia particles on the surface increases with the time and the electrolyte concentration. The reason was explained earlier.

Thickness of the layers was also measured by SEM cross section technique (images not shown here) and the corresponding results are presented in Table 3. Thicker layers were obtained when the processing time and the electrolyte concentration were increased. The electric current passing the electrochemical cell increases with the electrolyte concentration. As a consequence, more electrons are available on the anode surface and, hence, the electrochemical reactions are promoted leading to the formation of thicker layers.

Table 3
Thickness of layers for different growth conditions.

Nanoparticles concentration in electrolyte ($g\,l^{-1}$)	Process time (min)	
	5	10
0	11.5 μm	13.5 μm
0.5	–	14.5 μm
2	–	19 μm

3.3. Hardness

Vickers hardness values, obtained at 10 g for 10 s., of the composite layers grown under different conditions are presented in Fig. 6. It is worth mentioning that the surface hardness of the titanium substrates was determined to be ~190 Hv; therefore, the surface hardness of the substrates has been increases by a factor of three after the EEMAO treatment.

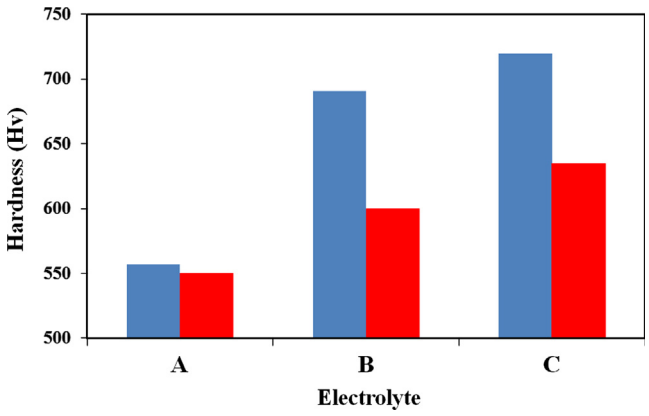

Fig. 6. Vickers hardness of the layers grown in different electrolytes (Red: 5 min and Blue: 10 min). (For interpretation of the references to color in this figure legend, the reader is referred to the web version of this article.)

It is also observed that the surface hardness increases with processing time as well as the zirconia concentration. One reason behind this behavior is increasing the zirconia content in the layers, as explained earlier. As the second reason, it is envisaged that the zirconia particles act as nucleation sites for anatase and rutile phases. As a consequence, higher number of energetically favorable sites for nucleation is available and, hence, more nuclei form at higher zirconia concentration leading to growth of structures with finer grains. Fine grain layers provide higher harnesses.

4. Conclusions

We employed EEMAO technique to grow TiO_2–ZrO_2 nanostructured composite coatings on titanium substrates where the surface harness of the titanium substrates was successfully increased from ~190 Hv to ~700 Hv. It was shown that the anatase/rutile and tetragonal/monoclinic zirconia rations increased with the processing time and the electrolyte concentration. The concentration of the zirconia phases also increased with time and concentration. SEM micrographs showed that the zirconia phase was evenly distributed in the titania matrix. The surface hardness of the TiO_2–ZrO_2 composite layers was observed to increase with the zirconia concentration. We proposed a processing-structure-properties correlation.

Acknowledgment

First author wishes to thank his family, particularly his father, because of their support in all steps of his life.

References

[1] J. Cheol Oh, D.K. Choo, S. Lee, Microstructural modification and hardness improvement of titanium-base surface-alloyed materials fabricated by high-energy electron beam irradiation, Surface and Coatings Technology 127 (2000) 76–85.

[2] Y. Huang, Y. Yan, X. Pang, Electrolytic deposition of fluorine-doped hydroxyapatite/ZrO_2 films on titanium for biomedical applications, Ceramics International 39 (2013) 245–253.

[3] Y. Tian, C. Chen, L. Chen, L. Chen, Study on the microstructure and wear resistance of the composite coatings fabricated on Ti–6Al–4V under different processing conditions, Applied Surface Science 253 (2006) 1494–1499.

[4] D. Vojtěch, T. Kubatík, M. Pavlíčková, J. Maixner, Intermetallic protective coatings on titanium, Intermetallics 14 (2006) 1181–1186.

[5] R. Roest, B.A. Latella, G. Heness, B. Ben-Nissan, Adhesion of sol–gel derived hydroxyapatite nanocoatings on anodised pure titanium and titanium (Ti6Al4V) alloy substrates, Surface and Coatings Technology 205 (2011) 3520–3529.

[6] L. Mohan, C. Anandan, V.K. William Grips, Corrosion behavior alloy Beta-21S coated with diamond like carbon in Hank's solution, Applied Surface Science 258 (2012) 6331–6340.

[7] W. Wang, M. Wang, Z. Jie, F. Sun, D. Huang, Research on the microstructure and wear resistance of titanium alloy structural members repaired by laser cladding, Optics and Lasers in Engineering 46 (2008) 810–816.

[8] I. Watanabe, M. McBride, P. Newton, K.S. Kurtz, Laser surface treatment to improve mechanical properties of cast titanium, Dental Materials 25 (2009) 629–633.

[9] A.C.L. Faria, R.C.S. Rodrigues, A.P.R.A. Claro, M.d.G.C. de Mattos, R.F. Ribeiro, Wear resistance of experimental titanium alloys for dental applications, Journal of the Mechanical Behavior of Biomedical Materials 4 (2011) 1873–1879.

[10] C. Richard, C. Kowandy, J. Landoulsi, M. Geetha, H. Ramasawmy, Corrosion and wear behavior of thermally sprayed nano ceramic coatings on commercially pure Titanium and Ti–13Nb–13Zr substrates, International Journal of Refractory Metals and Hard Materials 28 (2010) 115–123.

[11] A. Médevielle, F. Thévenot, D. Tréheux, Wear resistance of zirconias. Dielectrical approach, Wear 213 (1997) 13–20.

[12] S.T. Aruna, N. Balaji, K.S. Rajam, Phase transformation and wear studies of plasma sprayed yttria stabilized zirconia coatings containing various mol% of yttria, Materials Characterization 62 (2011) 697–705.

[13] R.V. Kurahatti, A.O. Surendranathan, S. Srivastava, N. Singh, A.V. Ramesh Kumar, B. Suresha, Role of zirconia filler on friction and dry sliding wear behaviour of bismaleimide nanocomposites, Materials and Design 32 (2011) 2644–2649.

[14] K.V.R. Chary, G.V. Sagar, D. Naresh, K.K. Seela, B. Sridhar, Characterization and reactivity of copper oxide catalysts supported on TiO_2–ZrO_2, Journal of Physical Chemistry B 109 (2005) 9437–9444.

[15] N.K. Sahoo, S. Thakur, R.B. Tokas, Superior refractive index tailoring properties in composite ZrO_2/SiO_2 thin film systems achieved through reactive electron beam codeposition process, Applied Surface Science 253 (2006) 618–626.

[16] A. Kitiyanan, S. Sakulkhaemaruethai, Y. Suzuki, S. Yoshikawa, Structural and photovoltaic properties of binary TiO_2–ZrO_2 oxides system prepared by sol–gel method, Composites Science and Technology 66 (2006) 1259–1265.

[17] I. Piwoński, K. Soliwoda, A. Kisielewska, R. Stanecka-Badura, K. Ka¸dzioła, The effect of the surface nanostructure and composition on the antiwear properties of zirconia–titania coatings, Ceramics International 39 (2013) 1111–1123.

[18] P. Sudhagar, S. Nagarajan, M. Mohana, V. Raman, T. Nishimura, S. Kim, Y.S. Kang, N. Rajendran, Nanocomposite coatings on biomedical grade stainless steel for improved corrosion resistance and biocompatibility, Applied Materials and Interfaces 4 (2012) 5134–5141.

[19] X. Miao, D. Sun, P.W. Hoo, J. Liu, Y. Hu, Y. Chen, Effect of titania addition on yttria-stabilised tetragonal zirconia ceramics sintered at high temperatures, Ceramics International 30 (2004) 1041–1047.

[20] J.M. Wheeler, C.A. Collier, J.M. Paillard, J.A. Curran, Evaluation of micromechanical behaviour of plasma electrolytic oxidation (PEO) coatings on Ti–6Al–4V, Surface and Coatings Technology 204 (2010) 3399–3409.

[21] M.R. Bayati, R. Molaei, A. Kajbafvala, S. Zanganeh, H.R. Zargar, K. Janghorban, Investigation on hydrophilicity of micro-arc oxidized TiO_2 nano/micro-porous layers, Electrochimica Acta 55 (2010) 5786–5792.

[22] M.R. Bayati, A.Z. Moshfegh, F. Golestani-Fard, In situ growth of vanadia–titania nano/micro-porous layers with enhanced photocatalytic performance by micro-arc oxidation, Electrochimica Acta 55 (2010) 3093–3102.
[23] A.L. Yerokhin, V.V. Lyubimov, R.V. Ashitkov, Phase formation in ceramic coatings during plasma electrolytic oxidation of aluminium alloys, Ceramics International 24 (1998) 1–6.
[24] A. Dey, R.U. Rani, H.K. Thota, A.K. Sharma, P. Bandyopadhyay, A.K. Mukhopadhyay, Microstructural, corrosion and nanomechanical behaviour of ceramic coatings developed on magnesium AZ31 alloy by micro arc oxidation, Ceramics International 39 (2013) 3313–3320.
[25] P. Sarkar, D. De, H. Rho, Synthesis and microstructural manipulation of ceramics by electrophoretic deposition, Journal of Materials Science 39 (2004) 819–823.
[26] L. Miao, S. Cai, Z. Xiao, Preparation and characterization of nanostructured ZnO thin film by electrophoretic deposition from ZnO colloidal suspensions, Journal of Alloys and Compounds 490 (2010) 422–426.
[27] A. Simchi, F. Pishbin, A.R. Boccaccini, Electrophoretic deposition of chitosan, Materials Letters 63 (2009) 2253–2256.
[28] I. Corni, M.P. Ryan, A.R. Boccaccini, Electrophoretic deposition: from traditional ceramics to nanotechnology, Journal of the European Ceramic Society 28 (2008) 1353–1367.
[29] S. Novak, K. König, Fabrication of alumina parts by electrophoretic deposition from ethanol and aqueous suspensions, Ceramics International 35 (2009) 2823–2829.
[30] E. Matykina, R. Arrabal, P. Skeldon, G.E. Thompson, Investigation of the growth processes of coatings formed by AC plasma electrolytic oxidation of aluminium, Electrochimica Acta 54 (2009) 6767–6778.
[31] H. Tong, F. Jin, L. Shen, Fabrication of porous ceramic coatings embedded nanograins on titanium alloys, Journal of the Korean Physical Society 46 (2005) S134–S136.
[32] K.M. Lee, Y.G. Ko, D.H. Shin, Incorporation of carbon nanotubes into micro-coatings film formed on aluminum alloy via plasma electrolytic oxidation, Materials Letters 65 (2011) 2269–2273.
[33] M. Aliofkhazraei, A.S. Rouhaghdam, Wear and coating removal mechanism of alumina/titania nanocomposite layer fabricated by plasma electrolysis, Surface and Coatings Technology 205 (2011) S57–S62.
[34] A.L. Yerokhin, A. Leyland, A. Matthews, Kinetic aspects of aluminium titanate layer formation on titanium alloys by plasma electrolytic oxidation, Applied Surface Science 200 (2002) 172–184.
[35] A.L. Yerokhin, X. Nie, A. Leyland, A. Matthews, S.J. Dowey, Plasma electrolysis for surface engineering, Surface and Coatings Technology 122 (1999) 73–93.
[36] D. Yoo, I. Kim, S. Kim, C. Hahn, C. Lee, S. Cho, Effects of annealing temperature and method on structural and optical properties of TiO_2 films prepared by RF magnetron sputtering at room temperature, Applied Surface Science 253 (2007) 3888–3892.
[37] A.W. Czanderna, C.N. Ramachandra Rao, J.M. Honig, The anatase-rutile transition. Part 1 Kinetics of the transformation of pure anatase, Transactions of the Faraday Society 54 (1958) 1069.
[38] J. Park, J.K. Heo, Y.C. Kang, The properties of RF sputtered zirconium oxide thin films at different plasma gas ratio, Bulletin of the Korean Chemical Society 31 (2010) 397.
[39] S. Wang, C. Liu, F. Shan, Structural investigation of the zirconium–titanium based amino trimethylene phosphonate hybrid coating on aluminum alloy, Acta Metallurgica Sinica (English Letters) 22 (2009) 161–166.
[40] F. Samanipour, M.R. Bayati, F. Golestani-Fard, H.R. Zargar, T. Troczynski, A. R. Mirhabibi, An innovative technique to simply fabricate ZrO_2–HA–TiO_2 nanostructured layers, Colloid Surfaces B 86 (2011) 14–20.
[41] M.R. Bayati, F. Golestani-Fard, A.Z. Moshfegh, How photocatalytic activity of the MAO-grown TiO_2 nano/micro-porous films is influenced by growth parameters?, Applied Surface Science 256 (2010) 4253–4259.
[42] M.R. Bayati, F. Golestani-Fard, A.Z. Moshfegh, The effect of growth parameters on photo-catalytic performance of the MAO-synthesized TiO_2 nano-porous layers, Materials Chemistry and Physics 120 (2010) 582–589.
[43] A. Rapacz-Kmita, A. Ślósarczyk, Z. Paszkiewicz, Mechanical properties of HAp–ZrO_2 composites, Journal of the European Ceramic Society 26 (2006) 1481–1488.